eJSE International
Electronic Journal of Structural Engineering 12(1) 2012

Comparative Study of Two Optimization Methods for Structural Damage Severity Estimation

W.L. Bayissa
Queensland University of Technology, Queensland, Australia

N. Haritos
The University of Melbourne, Victoria, Australia

ABSTRACT: This paper presents comparative assessment of the performance characteristics of two optimization algorithms, namely a deterministic nonlinear least squares (NLS) optimization and a stochastic adaptive simulated (ASA) annealing global optimization, implemented in the context of a two-stage structural damage severity estimation approach. First, both the standard NLS and global ASA optimization algorithms were employed to estimate single as well as multiple structural damage severity via minimization of a cost function expressed in terms of the scalar distance between the "damage-sensitive" response parameter determined from a potentially damaged structure and that computed from a finite element model of the undamaged structure. Consequently, the results obtained from extensive simulation studies conducted on data acquired from numerical experiments performed on a simply supported beam-like structure using both of the optimization algorithms in the presence of more realistic damage condition states were compared. The practical relevance of these results are critically summarized in this paper.

1 INTRODUCTION

In the past, various optimization techniques have been employed in the context of finite element model updating for structural damage severity estimation (Sohn et al. 2004, Mottershead & Friswell 1993). However, ill-conditioning and non-uniqueness problems are often encountered with the solution of inverse problems for determining the damage parameters of a model for given measured data due to factors such as measurement noise, modelling error, incompleteness of the measurement data, low level of sensitivity of the response parameters to localized damage, high-dimensionality and non-linearity. Various researchers have proposed powerful optimization techniques in order to overcome the ill-conditioning and non-uniqueness problems often encountered in finite element model parameter updating and subsequent damage severity estimation of large-scale structures (Jaishi et al. 2007, Jaishi & Ren 2007, Levin & Lieven 1998, Friswell et al. 1998). Multi-stage multi-objective optimization techniques have been proposed for finite element model updating in order to localize and quantify damage in large-scale structures subjected to severe damage condition states for damage identification in larger-scale structures (Perera & Ruiz 2008, 2007).

In order to overcome the aforementioned ill-conditioning difficulties, a two-stage damage identification strategy that combines non-model based and model-based damage identification approaches is proposed for structural damage detection, localization and severity estimation (Bayissa & Haritos 2009).

In this paper, the performance characteristics of a standard deterministic nonlinear optimization as well as a stochastic global optimization technique for solving the inverse problem (i.e., inverse identification of structural damage severity) when implemented in the context of a two-stage structural damage identification process are investigated. Damage localization information acquired from the first stage of the damage identification process is employed for quantification of damage severity via minimization of a cost function expressed in terms of a damage-sensitive statistical response parameter. Consequently, the comparative efficiency of the two optimization methods, namely the standard nonlinear least-squares and adaptive simulated annealing global stochastic optimization techniques, are systematically demonstrated on numerical experimental data obtained from a simply supported RC beam model subjected to a single as well as multiple damage condition states.

2 OPTIMIZATION ALGORITHMS FOR SEVERITY ESTIMATION

In this section, the theoretical background regarding structural damage severity prediction as conducted

using the two types of optimization technique in the context of two-stage structural damage identification approach are presented.

2.1 *Nonlinear least-squares optimization*

The nonlinear least-squares (NLS) optimization method employs the finite-differencing gradient based iterative search techniques which comprises of two main algorithms, namely Gauss-Newton and Levenberg-Marquardt (refer to MATLAB® User's manual, version 6.5). The routine *lsqnonlin* implemented in the MATLAB optimization toolbox is used to perform the nonlinear least-squares fit on the output of the objective function, which is defined in terms of the sum-of-squares of the scalar distance between the calculated and measured responses.

2.2 *Adaptive simulated annealing global optimization*

In general, simulated annealing (SA) algorithms are non-homogeneous variants of Monte Carlo importance-sampling techniques consisting of a "temperature" schedule for efficient sequential random searching and global optimization of non-convex and non-differentiable cost-functions (Kirkpatrick 1983). The long computation time required for execution of standard SA algorithms has prompted researchers to develop variants of SA that utilize a faster annealing schedule in order to satisfy the stopping criterion of the optimization function. The ASA algorithm is found to provide the best global fit to a nonlinear constrained non-convex cost-function over multi-dimensional space using an importance sampling technique. The algorithm permits an annealing schedule for "temperature" T decreasing exponentially in annealing-time and permits adaptation to changing sensitivities in the multi-dimensional parameter-space through introduction of re-annealing (Ingber 1993). The ASA algorithm is reported to have outperformed various global optimization methods and other variants of SA such as Boltzmann annealing and fast annealing (Ingber 1996).

In order to conduct global optimization of a cost-function coded in the MATLAB environment for the research performed in this paper, an open ASA source code written in the C-language (Ingber 1993) was utilized along with a MATLAB gateway function known as ASAMIN to create C MEX-files (http://www.igi.tugraz.at/lehre/MLA/WS01/asamin.html).

2.3 *Convergence Criteria*

In this study, the estimation of structural damage severity is conducted by implementing both NLS and ASA algorithms on a cost-function defined in terms of the sum-of-squares of the scalar distance between the calculated and measured MSV, given by:

$$\min_{\beta \in \Re^n} J(k) = \frac{1}{2} \sum_{j=1}^{N_d} \sum_{\delta r=1}^{N_{\delta r}} \left(\frac{\mu_j^{\delta r}}{\left\| \mu^{\delta r} \right\|} - \frac{\Gamma \mu_j^{\delta r}(k)}{\left\| \Gamma \mu^{\delta r}(k) \right\|} \right)^2 \quad (1)$$

where N_d is the number of measurement degrees of freedom, β is a set of structural model parameters, $N_{\delta r}$ are the number of frequency bandwidths used, $\mu_j^{\delta r}$ is the MSV obtained from the potentially damaged condition states at the j^{th} measurement grid point, $\mu_j^{\delta r}(k)$ is the MSV of the undamaged condition state at the j^{th} model degree of freedom, Γ is a mapping matrix that transforms the MSVs obtained for the full model degrees of freedom to those associated with the measurement grid points, only.

The general optimization process implemented for the quantification of structural damage include: initiation of the optimization variables (i.e. stiffness parameters); specification of the optimization parameter options; upper and lower limits for global optimization variables; calling the MATLAB gateway function, ASAMIN; calling the global optimization routine, ASA; calling the routine *lsqnonlin*; calling the finite element model based MATLAB function to compute the "damage-sensitive" response parameter (see Equations (8)-(11)); computation of the cost-function defined in Equation (1); and quantification of damage severity based on the optimal model parameter outputs of the converged and valid solution. The sequential flow diagram of the optimization process implemented for the estimation of damage severity is presented in Fig. 1.

In general, the structural equation of motion for a linearly vibrating damped multi-degree-of-freedom system subjected to arbitrary excitation forces can be described in a matrix form, as follows:

$$M\ddot{u}(t) + C\dot{u}(t)(K + \Delta K)u(t) = F(t) \quad (2)$$

where M, C, and K are the mass, damping and stiffness matrices, respectively, for pristine structural system. ΔK is the change in the stiffness matrix due to possible degradation in the structural condition. $\ddot{u}(t)$, $\dot{u}(t)$ and $u(t)$ are acceleration, velocity and displacement response vectors, respectively; F(t) is the excitation force vector.

In order to implement the proposed optimization tools, the structural model is first parameterized in terms of structural stiffness as an assembly of substructures or element stiffness matrices assuming that damage affects only the stiffness properties of the structure, as follows:

$$\overline{K} = K + \Delta K \quad (3)$$

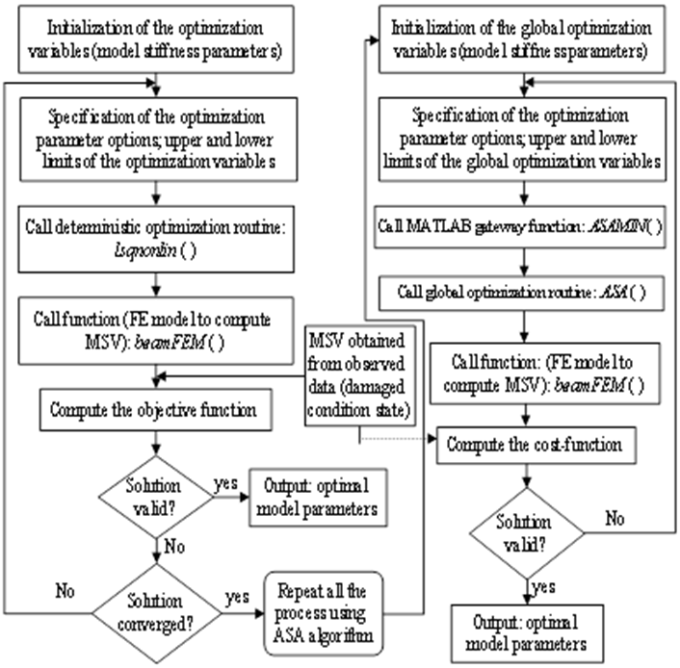

Figure 1. Flowchart of the optimization algorithms implemented.

where $\overline{\mathrm{K}}$ is the assembled global stiffness matrix with possible stiffness damage conditions. The stiffness degradation matrix can also be described in terms of the pristine structural element stiffness matrix, as follows:

$$\Delta \mathrm{K} = \sum_{j=1}^{nd} \mathrm{K}_j^e \, \delta k_j \tag{4}$$

where K_j^e is the stiffness matrix of the element (substructure) j that contributes to the global stiffness matrix. nd is the number of degraded elements; δk_j is the stiffness parameter degradation indicator for element e whose values need to be determined, $(0 \le \delta k_j \le 1)$, as follows:

$$\delta k_j = \frac{\overline{\mathrm{K}}_j^e}{\mathrm{K}_j^e} \tag{5}$$

where K_j^e and $\overline{\mathrm{K}}_j^e$ are the element stiffness matrices for pristine and degraded element e in the substructure j, respectively. In this study, the severity of stiffness degradation in the elements of various substructures is defined, as follows (refer to Equation (5)):

$$Dk_j = (1 - \delta k_j) = \frac{\Delta \overline{\mathrm{K}}_j^e}{\mathrm{K}_j^e} \equiv \frac{(\Delta EI)_j^e}{EI_j^e} \equiv \frac{\Delta E_j^e}{E_j^e} \tag{6}$$

where Dk_j represent the predicted degradation in substructure j. EI_j^e is the flexural rigidity for the pristine element e in the substructure j; $(\Delta EI)_j^e$ is the change in the flexural rigidity of element e in the substructure j. ΔE_j^e is the change in the material stiffness of element e in the substructure j and E_j^e is the material stiffness of the pristine element e for substructure j. The percentage of the prediction error, Err, is determined, as follows:

$$Err_j = \left(\frac{Dk_j^p - Dk_j^a}{Dk_j^a} \right) \times 100 \tag{7}$$

where Dk_j^p and Dk_j^a represent the predicted and the applied damage severity in substructure j, respectively.

2.4 *Damage-sensitive response parameters*

In the past, statistical parameters known as the mean square values (MSVs) of the vibration response signal and its derivatives have been identified as "damage-sensitive" parameters with significant advantages over commonly used non model-based damage identification methods (Loughlin & Cakrak 2000, Lutes & Larsen 1990, Bayissa et al. 2008). The salient features attributed to their use include sensitivity to local and global damage and strong physical relationships with key structural dynamic properties. The MSVs in the time, spectral, modal and wavelet domains, respectively, can be obtained, as follows (Bayissa & Haritos 2009, 2007, Bayissa et al. 2008):

$$\mu_r = r_{yy}(0) = \frac{1}{T}\int_0^T |y(t)|^2 dt = \frac{1}{N}\sum_{n=0}^{N-1} |y[t]|^2 \tag{8}$$

$$\mu_{ss} = \frac{1}{2\pi}\int_{-\infty}^{\infty} S_{yy}(\omega) d\omega = \frac{1}{2\pi}\int_{-\infty}^{\infty} |H(\omega)|^2 S_{PP}(\omega) d\omega \tag{9}$$

$$\mu_{\varphi} = \frac{1}{2\pi}[\varphi][\varphi]^T \int_{-\infty}^{\infty} H_r^*(\omega)[S_{PP}(\omega)][H_r(\omega)] d(\omega)[\varphi][\varphi]^T \tag{10}$$

$$\mu_{t,f}^0 = \int_{-\infty}^{\infty}\int_{-\infty}^{\infty} |Q(\alpha,\beta)|^2 \, dtdf \tag{11}$$

where μ_r, μ_{ss}, μ_{φ} and $\mu_{t,f}^0$ are the MSVs in the time, spectral, modal and wavelet domains, respectively. $y(t)$ is a time series signal, $y[t_n]$ is an N point sequence of $y(t)$, $r_{yy}(0)$ is the autocorrelation at zero time shift, T is the time period. $S_{yy}(\omega)$ is the response power spectral density (PSD), $H(\omega)$ is the frequency response function (FRF), $S_{pp}(\omega)$ is the excitation power spectral density, $[H_r(\omega)]$ is the diagonal matrix of the modal FRF, ω is the excitation frequency. $Q(\alpha,\beta)$ represents the coefficients of the wavelet transforms, in which α and β are the scale and translation parameters, respectively.

In this study, Equations (8)-(11) are employed for computation of the MSVs for damage severity esti-

mation studies conducted with both the NLS and ASA optimization algorithms.

3 NUMERICAL SIMULATION STUDIES

In this section, the NLS and ASA optimization techniques are demonstrated on the simply supported reinforced concrete beam shown in Fig. 2(a)-(b). The parameterized FE model of the beam is developed in a MATLAB toolbox (Ref. CALFEM 3.4 User's manual) and meshed using two-dimensional beam elements resulting in 25 elements. Both single and various types of multiple damage conditions are introduced with severity levels ranging from 1%–20%. The location and the severity level of the simulated damage conditions at each element location are presented in Table 1. The material properties for the undamaged beam include a Young's modulus of 30GPa, mass density of 2400 kg/m3 and Poisson's ratio of 0.25. Structural damage is simulated by reducing the material stiffness and the level of severity induced is directly related to the percentage reductions adopted, (refer to Equation (6)).

Table 1. Simulated structural damage conditions applied to the RC beam.

Applied structural damage conditions (%)			
Single damage condition	Multiple damage condition		
E7	E7	E13	E19
1	1	1	1
2	2	2	2
5	5	5	5
10	10	10	10
15	15	15	15
20	20	20	20
-	10	20	10
-	5	20	15

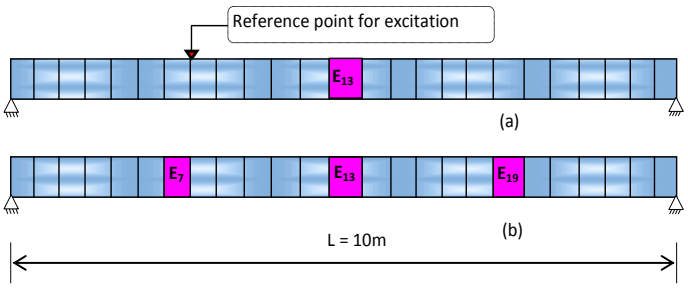

Figure 2. FE model for a simply supported beam with damage locations indicated: (a) single damage (at element 13); (b) multiple damage (at elements 7, 13 and 19).

In order to perform a comparative assessment of the robustness of the inverse damage severity estimation algorithms adopted, the following two sets of structural damage identification data were considered:

(i) An accurate numerical model and noise-free response data (full set of measurement grid points and complete set of modes);

(ii) An approximate numerical model and incomplete noisy response data (incomplete sets of both measurement grid points and modes).

3.1 *Using an accurate numerical model and noise-free response data*

In this section, an error-free numerical model and noise-free response data obtained at a full set of grid points (see Fig. 2) using the first 10 flexural modes (i.e., natural frequencies and mode shapes and a constant modal damping ratio of 0.01) are implemented for damage severity prediction. The number of degrees of freedom of the model and the simulated measurements were kept the same and a single frequency bandwidth (i.e., $N_{\delta r} = 1$) that encompassed the first 10 flexural modes was used for computation of the MSVs (see Equation (10)). Hence, the value of the transformation matrix for all degrees of freedom was taken to be 1, $\Gamma = [1,....,1]^T$. Finally, the MSVs obtained from the numerical experimental data were used along with the MSV computed from the FE model for the pristine structural condition state to solve the optimization problem (see Equation (1)). Consequently, the NLS and ASA optimization algorithms were employed to inversely predict the stiffness parameters for the different damage conditions.

The results for single and multiple damage severity estimations obtained using noise-free response data are presented in Figs. 3–6 and Figs. 7–9, for NLS and ASA optimization, respectively. These results demonstrate that the standard NLS optimization technique is able to accurately determine different levels of damage induced on the beam as shown in Fig. 3 (for the single damage condition), Fig. 4 (for spatially uniform multiple damage states) and Figs. 5 and 6 (for spatially non-uniform multiple damage states). Similarly, the ASA method is also found to accurately predict the single damage condition (Fig. 7), spatially uniform multiple damage states (Fig. 8) and spatially non-uniform multiple damage states (Fig. 9) induced on the beam. Even though the results shown are only for the 5% to 20% damage level for the purpose of clarity of the Figures, both methods were found to accurately estimate even the 1% damage level.

Therefore, these results shows that both the standard NLS and ASA global optimization methods can be used to accurately predict the structural damage severity in a two-stage damage identification procedure provided that the response data is free from measurement noise and the baseline numerical model is relatively accurate.

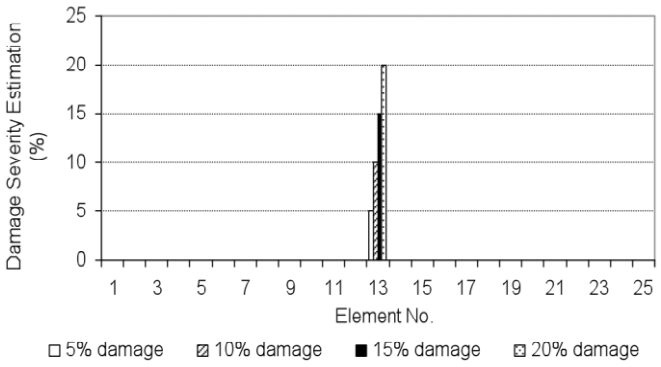

ure 3. Single damage severity estimation using NLS optimization.

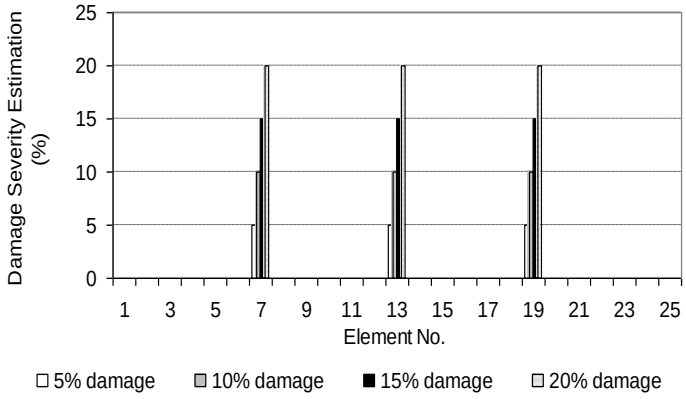

Figure 4. Multiple regular damage severity estimation using NLS optimization.

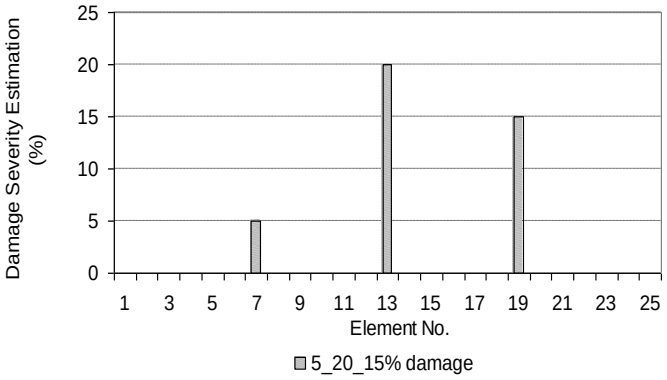

Figure 5. Multiple irregular damage severity estimation using NLS optimization.

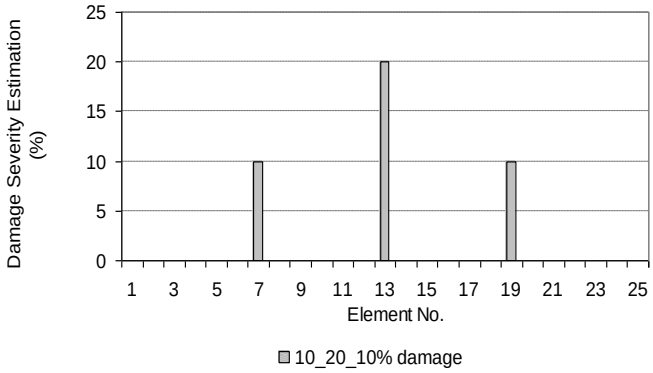

Figure 6. Multiple irregular damage severity estimation using NLS optimization.

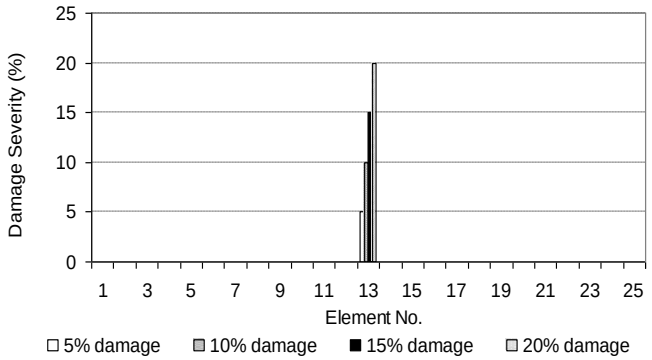

Figure 7. Single damage severity estimation using ASA optimization.

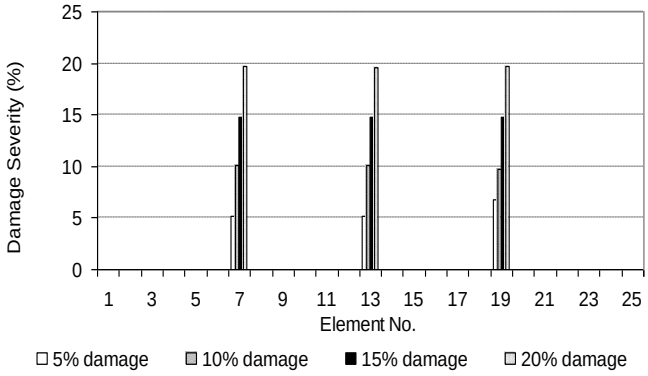

Figure 8. Multiple regular damage severity estimation using ASA optimization.

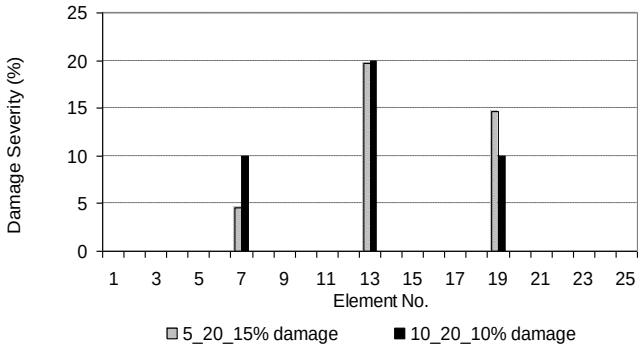

Figure 9. Multiple irregular damage severity estimation using ASA optimization.

3.2 *An approximate numerical model with incomplete and noisy response data*

The investigation conducted in this section simulates a more realistic scenario in structural damage identification problems, where incompleteness in both the measurement points and modes is often coupled with measurement noise and numerical model uncertainties.

In order to simulate these conditions, (a) MSVs were computed only at half of the beam model nodes (or 13 measurement grid points); (b) only half of the flexural modes (or 5 modes) that were used in the previous case (section 3.1) were employed for com-

putation of the MSVs using Equation (8); (c) Gaussian random noise with magnitude ranging from 1% to 20% were added to the numerically simulated structural response data series prior to computation of the MSVs. In Figs. 10 (a)–(c), the finite element model nodes, the grid points at which MSVs were obtained from the simulated measurement data, the location of the induced structural damage and the substructure elements of the spare measurement grid points of the beam are presented. Moreover, a typical response PSD implemented for computation of MSVs and subsequent damage severity estimation is shown in Fig. 11. Finally, the actual damage severity estimation studies were conducted. Results are presented in sections 3.3 and 3.4, respectively, for the NLS and ASA optimization methods.

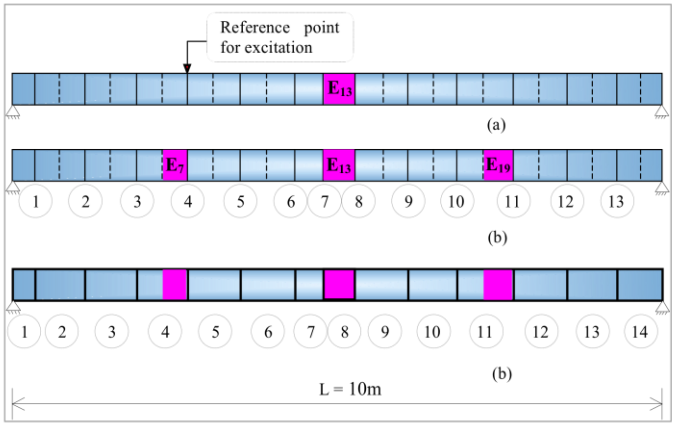

Figure 10. FE model of the beam with damage locations and simulated measurement grid points indicated: (a) single damage condition (at model element 13); (b) multiple damage condition (at model element 7, 13 and 19); (c) substructure model (damage is induced at substructure 4, 8 and 11).

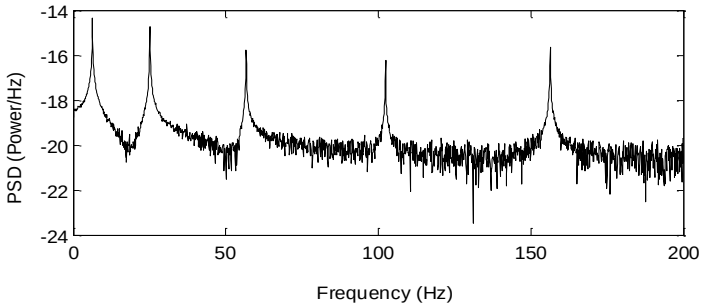

Figure 11. A typical response PSD with incomplete number of modes and 20% noise level ensemble averaged over 10 samples.

3.3 *Discussion on damage severity estimation results from NLS method*

In this section, the performance of the NLS damage severity estimation method is investigated for more practical damage scenarios and the results obtained are presented in Tables 2–7. For a single damage condition, the results obtained using NLS optimization show that this algorithm is capable of effectively predicting the level of damage (i.e., loss of stiffness) in the presence of significant noise levels, limited number of measurement grid points and incomplete vibration modes (Tables 2–4). The only exceptions are that for the very low 1% and 2% damage levels and the high 20% noise level, significant prediction errors of about 14% and 64%, respectively, were observed.

On the other hand, the multiple (regular) damage severity estimation results obtained using the NLS optimization algorithm presented in Tables 5–7, show a more favourable situation. For the 5% noise level, more accurate predictions were obtained for both the 15% and 20% multiple damage levels, and reasonably accurate severity estimations were obtained for the 5% multiple damage level. However, poor prediction results were obtained for the 10% multiple damage levels (Table 5). For the 10% noise level data, reasonably accurate prediction results were obtained for the 20% multiple damage condition while poor prediction results were obtained for 5%,-10%-15% multiple damage level state (Table 6). In the case of the 20% noise level data, prediction results with acceptable accuracy were obtained for 10% and 20% multiple damage levels while poor prediction results were obtained for the 5% and 15% multiple damage levels (Table 7).

Therefore, compared to the single damage condition, multiple damage severity conditions are found to affect the damage identification capability of the NLS optimization algorithm in the presence of measurement noise and incompleteness in the response data. Hence, the multiple damage severity estimation results presented reveal the limitations in the capability of the deterministic optimization technique and the accompanying significant increase in the number of iterations required for the optimization algorithm to converge to the global minimum and the susceptibility of the algorithm to converge to a local minimum (as opposed to the global minimum) as a result of the combined effects of measurement noise, incompleteness of the modal data and modeling uncertainty.

Consequently, it is suggested that the ASA stochastic global optimization algorithm can be implemented for identification of damage conditions in those cases where the deterministic NLS optimization method failed to provide accurate results.

The identification results when using the ASA optimization technique and the corresponding discussion are presented in section 3.4.

Table 2. Single damage severity estimation results for incomplete and 5% noise polluted response data.

Induced damage at Element 13 (E13)	Predicted damage at element 13 (E13)	No. of iterations	Prediction Error (%)
1	1.024	35	2.38
2	1.971	33	-1.44
5	5.170	37	3.39
10	10.125	34	1.25
15	15.080	32	0.53
20	20.040	35	0.20

Table 3. Single damage severity estimation results for incomplete and 10% noise polluted response data.

Induced damage at Element 13 (E13)	Predicted damage at element 13 (E13)	No. of iterations	Prediction Error (%)
1	1.058	44	5.83
2	1.935	38	-3.24
5	5.290	43	5.79
10	10.289	35	2.89
15	15.184	34	1.23
20	20.097	36	0.49

Table 4. Single damage severity estimation results for incomplete and 20% noise polluted response data.

Induced damage at Element 13 (E13)	Predicted damage at element 13 (E13)	No. of iterations	Prediction Error (%)
1	1.144	41	14.36
2	3.276	37	63.78
5	5.4406	44	8.81
10	10.589	41	5.89
15	15.388	74	2.59
20	20.227	32	1.14

Table 5. Multiple damage severity estimation results for incomplete and 5% noise polluted response data.

Induced damage at each element (Ei)			Predicted damage at each element (Ei)			No. of iterations	Prediction Error (%)		
E7	E13	E19	E7	E13	E19		E7	E13	E19
5	5	5	5.563	5.405	5.051	112	11.267	10.108	1.024
10	10	10	11.465	13.372	14.048	96	14.65	33.72	40.48
15	15	15	15.184	15.256	15.166	110	1.23	1.71	1.11
20	20	20	19.724	20.123	20.008	124	-1.38	0.62	0.04
10	20	10	10.088	20.236	9.897	109	0.88	1.18	-1.04
5	20	15	5.065	20.175	14.801	149	1.29	0.88	1.33

Table 6. Multiple damage severity estimation results for incomplete and 10% noise polluted response data.

Induced damage at each element (Ei)			Predicted damage at each element (Ei)			No. of iteration	Prediction Error (%)		
E7	E13	E19	E7	E13	E19		E7	E13	E19
5	5	5	6.598	6.271	5.401	113	31.96	25.42	8.02
10	10	10	11.167	13.606	14.026	121	11.674	36.06	40.26
15	15	15	19.678	19.820	20.007	126	31.188	32.14	33.38
20	20	20	20.438	20.529	19.806	133	2.19	2.65	-0.97
10	20	10	15.363	24.544	15.616	138	53.63	22.77	56.16
5	20	15	11.037	24.409	19.741	114	120.74	22.05	31.40

Table 7. Multiple damage severity estimation results for incomplete and 20% noise polluted response data.

Induced damage at each element (Ei)			Predicted damage at each element (Ei)			No. of iterations
E7	E13	E19	E7	E13	E19	
5	5	5	8.687	8.403	6.784	119
10	10	10	10.199	10.987	9.682	108
15	15	15	20.952	20.364	19.567	87
20	20	20	21.95	22.72	20.25	104
10	20	10	16.127	25.798	15.345	65
5	20	15	11.572	25.522	19.522	99

Prediction Error (%)		
E7	E13	E19
73.73	68.06	35.69
1.99	9.87	-3.19
39.68	35.76	30.44
9.73	13.62	1.23
61.27	28.99	53.45
131.44	27.61	30.15

3.4 *Discussion on damage severity estimation results from ASA method*

In this section, the robustness of the ASA damage severity estimation algorithm (as compared to that of NLS algorithm) is investigated in the presence of incomplete and noisy response data. With this aim in mind, the ASA global optimization was applied to the identification of multiple damage conditions where the standard NLS optimization was found to be ineffective; the results obtained are presented in Tables 8–10.

In general, when compared to the results obtained using NLS optimization discussed in the previous section 3.3, the ASA method is found to provide significantly more accurate damage severity predictions. For instance, for the 5% noise level and 10% multiple damage condition, the maximum prediction errors observed for ASA and NLS optimization methods are about 5.6% (Table 8) and 40.5% (Table 5), respectively. Similarly, for the 10% and 20% noise levels, the results obtained from the ASA algorithm are found to be more accurate than those obtained from the NLS algorithm (see Tables 9 and 10). For a 10% noise level and the 10% multiple damage condition, the maximum prediction error observed for ASA and NLS optimization methods are about 8.4% (Table 9) and 40.3% (Tables 6), respectively. For the 10% noise level and 15% multiple damage condition, the maximum prediction error observed for the ASA and NLS optimization methods are about 1.7% (Table 9) and 33.4% (Table 6), respectively.

Table 8. Multiple damage severity estimation results for incomplete and 5% noise polluted response data (ASA).

Induced damage at each element (Ei)			Predicted damage at each element (Ei)			No. of states generated (accepted)
E7	E13	E19	E7	E13	E19	
10	10	10	9.934	9.915	9.438	2171 (500)

Prediction Error (%)		
E7	E13	E19
-0.67	-0.85	-5.62

Table 9. Multiple damage severity estimation results for incomplete and 10% noise polluted response data (ASA).

Induced damage at each element (Ei)			Predicted damage at each element (Ei)			No. of states generated (accepted)
E7	E13	E19	E7	E13	E19	
10	10	10	9.888	10.058	9.162	1668 (400)
15	15	15	15.198	15.306	14.751	3270 (800)
10	20	10	10.162	20.507	9.713	2304 (500)
5	20	15	6.644	21.429	16.129	4555 (1000)
10	10	10	9.888	10.058	9.162	1668 (400)

Prediction Error (%)		
E7	E13	E19
-1.13	0.58	-8.38
1.32	2.04	-1.66
1.62	2.53	-2.87
32.88	7.14	7.52
-1.13	0.58	-8.38

Similarly, for the 20% noise level and various damage condition states, significant improvements in the severity estimation results were observed for the ASA algorithm as compared with those obtained from NLS optimization (see Table 10). Only for the 5% multiple damage condition and 20% noise, were there high level prediction errors observed from the ASA algorithm due to the effect of the reduction in the number of measurement grid points and vibration modes and also due to the less severe nature of the damage simulated. For the 15% multiple damage condition, the maximum prediction errors observed for the ASA and NLS optimization methods are about 1.8% (Table 10) and 30.4% (Tables 7), respectively. For irregular multiple damage (10%-20%-10%), the maximum prediction errors observed for the ASA and NLS optimization methods are about 7.2% (Table 10) and 53.5% (Tables 6), respectively. Similarly, for irregular multiple damage (5%-20%-15%), the maximum prediction error observed for the ASA and NLS optimization methods are about 5.5% (Table 10) and 30.2% (Table 7), respectively.

Table 10. Multiple damage severity estimation results for incomplete and 20% noise polluted response data (ASA).

Induced damage at each element (Ei)			Predicted damage at each element (Ei)			No. of states generated (accepted)
E7	E13	E19	E7	E13	E19	

5	5	5	8.687	8.403	6.784	4000 (880)
15	15	15	15.567	15.778	15.778	1149 (300)
10	20	10	10.209	20.973	9.277	2166 (500)
5	20	15	7.201	22.027	15.830	4615 (900)

Prediction Error (%)		
E7	E13	E19
73.74	68.06	35.67
3.78	5.19	-1.81
2.10	4.86	7.24
44.02	10.14	5.53

Overall, significant improvements have been able to be achieved by using the ASA algorithm over the NLS optimization method, in this example structure. The randomized global optimization method is more powerful for predicting structural damage severity than the deterministic search method when more realistic damage conditions and measurement noise are taken into consideration.

Finally, it can be concluded that the two-stage damage identification approach along with the ASA global optimization are found to be a powerful tool for accurately predicting structural damage severity in the presence of simulated complex damage condition states; significant measurement noise and incomplete modal data. The wide-ranging merits of the ASA global optimization approach when compared to those of the deterministic NLS method are however only realized at a price - the significantly longer processing time required to implement it.

4 CONCLUSIONS

In this paper, the performance characteristics of the nonlinear deterministic and global stochastic optimization techniques for solving the inverse problem (i.e., inverse estimation of structural damage severity) when implemented in the context of a two-stage structural damage identification process on a damaged beam have been extensively studied. In general, the results obtained from both algorithms studied show impressive performance of the two-stage structural damage identification approach despite the presence of modeling and measurement uncertainties and moderate levels of induced damage severity.

The deterministic nonlinear least-squares optimization technique was found to be quite efficient and accurate in predicting structural damage severity provided that there is no significant measurement noise. However, for cases involving data capture with higher levels of noise and a beam with multiple damage condition states, the nonlinear least-squares optimization technique was found to be ineffective and failed to converge to the true values of the model parameters. On the other hand, the adaptive simulated annealing global optimization method was found to be more robust and superior in its performance in finding the global optimal solution in the presence of significant noise levels and more complex multiple damage condition scenarios. Whilst offering significant merits, the adaptive simulated annealing method was however found to be computationally intensive, taking several processing hours on a standard PC computer before converging to the true values of the model parameters., It is therefore deemed prudent to consider applying both the deterministic nonlinear least-squares optimization technique as well as the ASA method for solution of inverse problems (damage severity estimation in this case) depending upon the nature and complexity of the problem concerned.

Finally, the results presented in this paper show that there are some variations observed in the accuracy levels of the damage severity estimation results and the time required for the optimization algorithms to converge due to the influence of incompleteness and measurement noise in the simulated response data. This influence is found to affect the prediction capability for multiple damage severity more so than for the single damage condition state.

5 PREFERENCES

ASAMIN User's Manual Version 1.33 (http://www.econ.ubc.ca/ssakata/ public_html/software/).

Bayissa. W. L., and Haritos, N., "Structural damage identification using a global damage identification technique", *International Journal of Structural Stability and Dynamics*, Vol. 9, 2009, pp 745-763.

Bayissa, W. L., and Haritos, N., "Damage identification in plate-like structures using bending moment response power spectral density", *Structural Health Monitoring*, Vol. 6, 2007, pp 5–24.

Bayissa, W. L, Haritos, N., and Thelandersson, S., "Vibration-based structural damage identification using wavelet transform", *Mechanical Systems and Signal Processing*, Vol. 22, 2008, pp 1194-1215.

CALFEM 3.4 User's Manual. *A Finite element toolbox*. Department of Structural Mechanics, Lund University, Sweden.

Friswell, M. I., Penny, J. ET., and Garvey, S. D., "A combined genetic and eigensensitivity algorithm for the location of damage in structures", *Computers and structures*, Vol. 68, 1998, pp 547–556.

Ingber, L., "Adaptive simulated annealing (ASA)", Caltech Alumni Association, Pasadena, CA, 1993. (http://www.alumini.caltech.edu/~ingber/).

Ingber, L., "Adaptive simulated annealing (ASA): Lessons learned", *Journal of Control and Cybernetics*, Vol. 25, 1996, pp 33–54.

Jaishi, B., Kim, H., Kim, M. K., Ren, W. X., and Lee, S., "Finite element model updating of concrete-filled steel tubular arch bridge under operational condition using modal flexibility", *Mechanical Systems and Signal Processing*, Vol. 21, 2007, pp 2406–2426.

Jaishi, B., and Ren, W.X., "Finite element model updating eigenvalue and strain energy residuals using multiobjective optimisation technique", *Mechanical Systems and Signal Processing*, Vol. 21, 2007, pp 2295–2317.

Kirkpatrick, S., Gelatt Jr, C.D., and Vecchi, M. P., "Optimization by simulated annealing, Science, Vol. 220, 1983, pp 671–680.

Levin, R. I., and Lieven, N. A., "Dynamic finite element model updating using simulated annealing and genetic algorithm", *Mechanical Systems and Signal Processing*, Vol. 12, 1998,pp 91–120.

Loughlin, P., and Cakrak, F. "Conditional moments analysis of transients with application to helicopter fault data", *Mechanical Systems and Signal Processing*, Vol. 14, 2000, pp 511-522.

Lutes, L. D., and Larsen, C. E., "Improved spectral method for variable amplitude fatigue prediction", *Journal of Structural Engineering*, Vol. 116, 1990, pp 1149-1164.

MATLAB 6.5 User's Manual Release 13 (2002). The Mathworks, Inc., Natick, MA, USA.

Mottershead, J. E., and Friswell, M. I., "Model updating in structural dynamics: A survey", *Journal of Sound and Vibration*, Vol. 167 1993, pp 347-375.

Perera, R., and Ruiz, A., "A multistage FE updating procedure for damage identification in large-scale structures based on multiobjective evolutionary optimization", *Mechanical Systems and Signal Processing*, Vol. 22, 2008, pp 970–991.

Perera, R., and Ruiz, A., "An evolutionary multiobjective framework for structural damage localization and quantification", *Engineering Structures*, Vol. 29, 2007, pp 2540–2550.

Sohn, H., Farrar, C. R., Hemez, F. M., Shunk, D. D., Stinemates, D. W., Nadler, B.R., and Czarnecki, J. J., "A review of structural health monitoring literature: 1996-2001", Los Alamos National Laboratory Report, 2004, LA-13976-MS.